

# **Gallium Electromagnetic (GEM) Thruster Concept and Design**

**Kurt A. Polzin and Thomas E. Markusic**

*NASA-Marshall Space Flight Center  
Huntsville, AL 35812*

**Rodney L. Burton and Robert E. Thomas**

*Department of Aerospace Engineering  
University of Illinois at Urbana-Champaign  
Urbana, IL 61801*

**David L. Carroll**

*CU Aerospace, LLC  
Champaign, IL 61820*

AIAA-2006-4652

## **Abstract:**

The element gallium appears attractive as a liquid metal propellant for electromagnetic thrusters. The system advantages and disadvantages of gallium are discussed, and performance predictions are presented for a gallium electromagnetic (GEM) thruster. Because of its low ionization potential ( $\phi_i = 6.0$  eV), the GEM thruster is predicted to have an efficiency of 70% at 4000 s specific impulse, and a high thrust density enabling a low specific mass for high power operation.

# Gallium Electromagnetic (GEM) Thruster Concept and Design

Kurt A. Polzin\* and Thomas E. Markusic\*

NASA-Marshall Space Flight Center  
Huntsville, AL 35812

Rodney L. Burton† and Robert E. Thomas‡

Department of Aeronautical and Astronautical Engineering  
University of Illinois at Urbana-Champaign  
Urbana, IL 61801

David L. Carroll

CU Aerospace, LLC  
Champaign, IL 61820

AIAA-2006-4652§

July 9-12, 2006

The element gallium appears attractive as a liquid metal propellant for electromagnetic thrusters. The system advantages and disadvantages of gallium are discussed, and performance predictions are presented for a gallium electromagnetic (GEM) thruster. Because of its low ionization potential ( $\phi_i = 6.0$  eV), the GEM thruster is predicted to have an efficiency of 70% at 4000s specific impulse, and a high thrust density enabling a low specific mass for high power operation.

## I. INTRODUCTION

A number of electric thrusters have used metallic elements as propellants in the past. These have included lithium-fed magnetoplasmadynamic (MPD) thrusters[1, 2], mercury[3, 4], cesium[5, 6] and indium-fed[7] electrostatic thrusters (ion engines and field emission electric propulsion), and bismuth-fed Hall thrusters[8–10]. Recently, Markusic *et al.* proposed a two-stage high-energy pulsed electromagnetic thruster design[11] that could employ liquid gallium as a propellant[12]. That design was motivated by a desire to produce a high-energy ( $\sim 10$  kJ/pulse), high-power ( $> 100$  kW) thruster that could deliver both high efficiency ( $> 50\%$ ) and high specific impulse ( $I_{sp} \sim 7500$  s).

To date, gallium has never been used as a propellant in any type of electric thruster, yet it has distinct advantages, particularly for high-power, electromagnetic propulsion. In addition, the use of gallium in conjunction with a two-stage accelerator design has the potential to address and alleviate several life-limiting *critical issues* in pulsed electromagnetic accelerator technology[11]. In the present

paper, we describe recent efforts at both NASA-Marshall Space Flight Center (MSFC) and the University of Illinois at Urbana-Champaign (UIUC) aimed at exploring and confirming the apparent advantages of using gallium.

In the next section, we review the speculated advantages of using gallium. We present several analyses aimed at validating the proposed advantages of a gallium thruster in Sect. III. Test hardware that will be used at both UIUC and MSFC to experimentally demonstrate the benefits of a gallium thruster is discussed in Sect. IV.

## II. MOTIVATION AND ADVANTAGES

### A. Properties of Gallium

The physical properties of gallium lead us to believe that it may be a very good propellant option in an electromagnetic accelerator. The most beneficial of these properties are as follows.

*1. Non-toxic and easily handled:* The element gallium is a coal and bauxite processing by-product. It is also thought to be relatively safe and easy to handle. Toxicity has doomed other promising liquid metal propellants (e.g., mercury, cesium) because of the hazards associated with laboratory testing and environmental contamination. Similarly, some attractive metallic propellants, such as lithium, are highly reactive and pose a fire and explosion hazard. The ease with which we can handle gallium should greatly simplify testing and validation procedures relative to the more reactive metals listed above. While gallium does al-

\*Member AIAA.

†Professor. Associate Fellow AIAA.

‡Graduate Research Assistant. NASA-Graduate Student Research Program Fellow. Member AIAA.

§Presented at the 42<sup>nd</sup> AIAA/ASME/SAE/ASEE Joint Propulsion Conference and Exhibit, Sacramento, CA. This material is declared a work of the U.S. Government and is not subject to copyright protection in the United States.

loy with and dissolve some metals (copper, aluminum), we have found that 316L stainless steel contains it quite well.

**2. Storability:** Gallium has a density of 5.91 kg/liter (versus xenon's 5.9 gm/liter at STP), a melting point of 30 °C, and a boiling point of 2400 °C. It may be stored as either a solid or dense liquid, requiring only minimal tankage. The temperature range over which gallium remains a liquid implies that minimal thermal management is required, and any leakage or boiloff losses should be negligible. The relatively high density leads to low storage volume, and propellant flow rates can be controlled using electromagnetic pumps[13].

**3. Ionization potential:** The first ionization potential of gallium is 6.0 eV while the second ionization potential is 20.5 eV. This implies that the plasma can remain singly ionized, minimizing the losses associated with the creation of multiply-charged ions.

**4. High molecular weight:** The molecular weight of gallium is 69.7 gm/mole, which, when combined with the low first ionization potential, helps to predict low frozen flow and sheath losses; the primary loss mechanisms in an electromagnetic thruster.

To get a rough comparison of various electromagnetic thruster propellants, we calculate a figure-of-merit (FOM), based on the assumption that both sheath losses and ionization frozen flow loss are proportional to the ionization potential of the propellant  $\phi_i$ . The FOM is defined as:

$$\text{FOM}_{4000} = \frac{\text{particle KE at } 4000 \text{ s } I_{sp}}{\text{particle energy of ionization}}.$$

Several values of the FOM are plotted in Table I.

Gallium's low ionization potential makes it relatively easy to generate a highly ionized plasma through electron impact ionization. Saha equilibrium curves showing the degree of ionization as a function of temperature and pressure are presented in Fig. 1. We observe that a 99% ionization fraction can be achieved at a pressure of 10 kPa when the temperature is only 12000 K ( $\sim 1$  eV). At this temperature, second ionization is minimal, as are the radiation losses. If the ion cost is equal to 5 times the

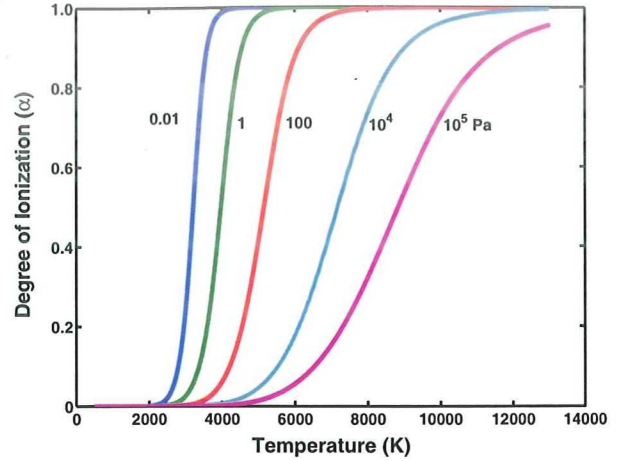


FIG. 1: Saha equilibrium calculation showing degree of ionization of gallium as a function of temperature and pressure.

ionization potential, which is consistent with other arc discharge thrusters, then we expect an ionization efficiency of 90-95%.

## B. Mitigation of 'Critical Issues'

In our two-stage accelerator, called the Gallium Electromagnetic (GEM) thruster and shown conceptually Fig. 2, liquid gallium is pumped through a porous tungsten electrode, coating the surface in a thin layer of liquid. A pulsed discharge (10-50 J/pulse) in the first stage vaporizes and ionizes the liquid gallium surface layer, ejecting it into the second stage and expanding it radially through a combination of gasdynamic and electromagnetic forces. The mass

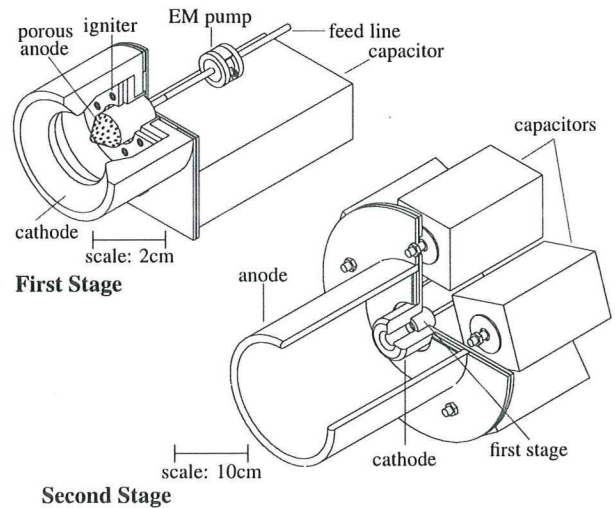


FIG. 2: Schematic illustrations of the first and second stages of a two-stage gallium electromagnetic thruster.

TABLE I: Propellant Figures of Merit  $[\text{KE}/\phi_i]$  at 4000s  $I_{sp}$ .

Prop.	Thruster	Mol. Wt.	Ioniz. Pot. [eV]	KE at 4000 s [eV]	FOM <sub>4000</sub>
Bismuth	TAL/Hall	209	7.3	1679	230
<b>Gallium</b>	<b>PPT/MPD</b>	<b>70</b>	<b>6.0</b>	<b>560</b>	<b>93</b>
Xenon	Ion, Hall	131	12.1	1055	87
Krypton	Ion, Hall	84	14.0	673	48
Argon	MPD	40	15.8	321	20
Lithium	MPD	7	5.4	55	10
Nitrogen	MPD	14	14.5	112	8
Hydrogen	MPD	1	13.6	8	<1

bit is varied by adjusting the first-stage discharge energy. In the second stage, a high energy ( $\mathcal{O}(100\text{-}1000)$  J/pulse) discharge begins once the gallium plasma from the first stage reaches the outer electrode, effectively “shorting” it to the inner electrode. A current sheet forms and the Lorentz force accelerates most of the propellant in the axial direction. A smaller amount of propellant is envisioned to pinch towards the center of the thruster, in a manner similar to a dense plasma-focus device. This pinched plasma column will be extruded as the current sheet propagates axially, forming a “virtual” center electrode that electrically connects the main current sheet to the rest of the circuit. If the current pulse lasts longer than the initial current sheet acceleration phase, the discharge should transition to that found in the quasi-steady MPD thruster mode of operation.

The design and operational characteristics of the GEM thruster have the potential to directly address critical issues that have hampered previous pulsed plasma accelerator development efforts (both for short pulse lengths and pulsed, quasi-steady operation). More specifically, the issues we seek to address are:

1. *Electrode erosion:* The high temperature levels inherent to arc discharges cause evaporation, and consequently long-term degradation, of the metallic electrodes. The GEM thruster first stage is designed to use electrode erosion as an intrinsic aspect of its operation rather than accepting it as an unavoidable, detrimental side effect. Since both the current conduction path and the propellant source are the molten metal covering the electrode surface, we are, in essence, using electrode erosion products as the propellant. In this way, the integrity of the underlying electrode material is maintained.

2. *Propellant injection:* The GEM thruster electrode sputters to inject propellant. This injection mode eliminates a pulsed valve, which would be very hard-pressed to operate reliably for  $10^{10}$  pulses with  $100\text{ }\mu\text{s}$  pulses in a high temperature environment. As previously demonstrated with the Teflon-fed pulsed plasma thruster[14], the mass bit can be controlled by changing either the geometry of the thruster at the backplate or the discharge current in the first stage.

3. *Current switching:* Gas-fed pulsed plasma thrusters (GF-PPTs) and quasi-steady MPD thrusters require a high-speed, high-current switch to electrically isolate the discharge chamber from a capacitor bank prior to discharge initiation. As with the valves, the performance requirements on the high-current switches are strenuous: current rise rates of  $\mathcal{O}(10^{11})$  A/sec, peak current levels of  $\mathcal{O}(10^4\text{-}10^5)$  A and lifetimes of  $\mathcal{O}(10^9\text{-}10^{10})$  pulses. Current state of the art switches, including solid state devices, cannot meet these specifications. The demands for a high-current switch are alleviated in the two-stage scheme, where the lower energy, lower current ( $\mathcal{O}(10^2\text{-}10^3)$  A) first-stage pulse can be switched using current state of the art technology. The high-energy second stage is self-switched when the gallium plasma from the first stage bridges the gap between the inner and outer electrodes.

4. *Facility requirements:* Another beneficial property of gallium is that it exists as a low vapor pressure liquid over a wide range of temperature ( $30\text{-}2400\text{ }^\circ\text{C}$ ), which means that it can be condensed (pumped) on simple, water-cooled plates during thruster testing under vacuum. This type of system can be operated at relatively low-cost (both in terms of facility and propellant cost) for long periods of time. This is a significant advantage when compared to the facility requirements and costs associated with operating large cryopumps for lifetime testing and validation of high-power, gas-fed thrusters (e.g. xenon-fed Hall thrusters) for long duration (e.g. ten year) missions.

### C. Development Level

The electromagnetic thruster was one of the earliest electric propulsion devices to be developed, originating from the so-called Marshall gun[15] used in fusion research during the 1950s, and flying on the Russian Zond Mars probe in 1964[14]. Rosebrock *et al.* successfully produced and accelerated a cadmium/zinc metal plasma[16]. Researchers at General Electric (GE) carried out the most extensive GF-PPT development program, producing several generations of electromagnetic thrusters[17–19]. Figure 3 shows performance data from their model A7 thruster. The thruster used xenon propellant and was pulsed at 5 Hz. The measurements indicate  $\eta_t \sim 50\text{-}80\%$  for corresponding  $I_{sp} \sim 5000\text{-}7000$  sec. The  $\mathbf{j} \times \mathbf{B}$  acceleration mechanism of the higher-energy GEM thruster is similar to the GE thrusters, so this data provides some experimental basis for the projected performance of the GEM thruster.

The GEM thruster uses a completely different propellant injection scheme than the GE thruster. There is however, some precedent for the GEM thruster two-stage accel-

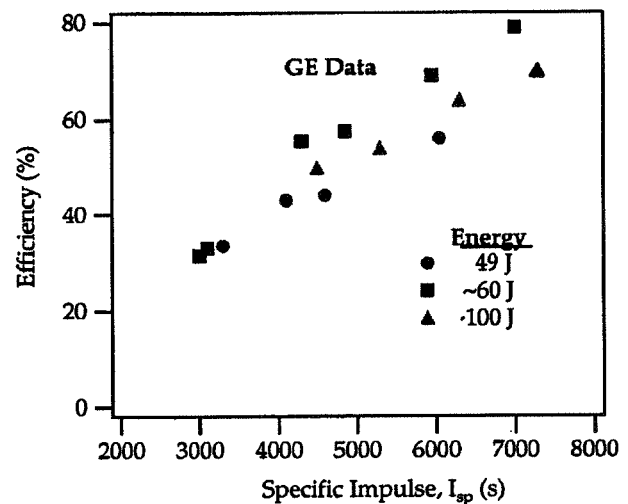


FIG. 3: Performance of the General Electric model A7 gas-fed PPT.

ation strategy. Turchi *et al.*[20] used an ablative Teflon plasma injector as the first stage of a rectangular-geometry two-stage accelerator and Gomilka *et al.*[21] used the ablation of a solid cadmium electrode in a two-stage coaxial device.

#### D. Acceleration Modes

There are three possible  $\mathbf{j} \times \mathbf{B}$  acceleration modes in high-power electromagnetic thruster applications. The snowplow mode, where the thruster barrel is initially filled with cold vapor and a current sheet acting as an electromagnetic shock accelerating through the gas, is a low efficiency acceleration mechanism. Unfortunately, the snowplowed plasma stagnates in the shock frame with a temperature of  $\sim 100$  volts and this thermal energy is lost as frozen flow in the exhaust process. In addition, the shocked, dense high temperature plasma has been shown to acquire a radial velocity, striking the electrodes. The slug mode, used in the GE-A7 PPT and the Pulsed Inductive Thruster (PIT)[22], ionizes all of the propellant in a few  $\mu\text{s}$  and accelerates it as a single mass, also in a few  $\mu\text{s}$ . Because the slug mode pulse is necessarily short ( $\sim 10 \mu\text{s}$ ) to prevent the gas from expanding downstream and setting up the snowplow mode, for a peak pulse power of 10 MW the maximum energy that can be delivered is on the order of 100 J/pulse. Thus 1000 Hz pulse repetition rates are needed to reach even 100 kW power levels. We regard 1000 Hz pulse frequencies as problematic, because vapor liberated from the walls during a pulse then only has 1000  $\mu\text{s}$  to evacuate the second stage chamber before the next pulse. Thrusters operating at higher power levels would require even less time to prepare for the next pulse.

The deflagration mode, demonstrated in the deflagration gun[23] and the gas-fed MPD thruster[24], does not suffer from the difficulties found in the snowplow and slug acceleration modes. A deflagration mode thruster can run at a pulse length between 50-500  $\mu\text{s}$ , greatly reducing the pulse rate for high-power operation. The deflagration mode employs a stationary  $\mathbf{j} \times \mathbf{B}$  force distribution, with the propellant fed from the back, ionized, and then pumped through the current sheet in a relatively efficient acceleration process.

### III. GEM THRUSTER ANALYSIS

#### A. Efficiency and Performance Evaluation

The efficiency and performance of the GEM thruster can be estimated using techniques developed for other electromagnetic thrusters. Estimating the thrust and  $I_{sp}$  are relatively straightforward. It has been well documented[24] that the thrust can be closely estimated by the relation:

$$T = (1 + e) \frac{L' I^2}{2} \quad [\text{N}]$$

where  $I$  is the thruster current in amperes,  $L'$  is the inductance per unit length, which is typically 0.3-0.5 F/m for coaxial systems, and  $e$  is a small factor, typically  $\sim 0.05$ , to account for additional electrothermal contributions to the thrust. Assuming  $e$  is zero, the specific impulse is the time-averaged value of  $L' I^2 / 2$  divided by the time-averaged weight throughput rate of propellant.

The estimate of efficiency is more difficult, but we have found it useful to consider the efficiency as a product of several factors[25]:

$$\text{overall efficiency } \eta = \eta_{\text{ppu}} \eta_t,$$

$$\eta_t = \eta_{\text{trans}} \eta_{\text{sheath}} \eta_{\text{ff}} \eta_{\text{div}} \eta_{\text{dist}}.$$

**Thrust efficiency**  $\eta_t = T u_e / 2 P_{in}$ : ability of thruster to convert input electrical power into thrust.

**Transfer efficiency**  $\eta_{\text{trans}}$ : fraction of energy not lost in capacitors, switching and lines between the PPU and the thruster.

**Sheath efficiency**  $\eta_{\text{sheath}}$ : energy fraction deposited in bulk plasma that is not transferred as heat to electrodes or walls.

**Frozen flow efficiency**  $\eta_{\text{ff}}$ : fraction of directed kinetic energy over total energy (including thermal and ionization energy) deposited in the flow.

**Divergence efficiency**  $\eta_{\text{div}}$ : accounts for thrust loss due to exhaust beam expansion.

**Distribution efficiency**  $\eta_{\text{dist}}$ : accounts for reduction in thrust due to non-monoenergetic exhaust energy distribution ( $\sim 1$  for ion thrusters).

Estimates of these efficiency factors are shown in Table II. Here, the gallium ion kinetic energy equivalent to an  $I_{sp}$  of 4000s is  $V=560$  volts. Based on MPD[24], PPT[14] and arcjet[26] experience, we have estimated the total sheath voltages as 8 times the ionization potential  $\phi_i = 6$  eV, which includes flow and electron losses to the walls. The frozen flow enthalpy is taken as 3 times the ionization potential. For the distribution efficiency we assume a relatively flat velocity profile and 10% slower neutrals by loss of ions from charge exchange, as was seen by Karras for xenon[19]. Finally the divergence efficiency is high due to the expected small beam expansion of 15 degrees[19]. Based on these estimations, the thrust efficiency of a GEM thruster can be as high as 73% and the overall efficiency with PPU conversion losses can reach 70%.

TABLE II: Efficiency of a GEM thruster at 4000s  $I_{sp}$ .

Efficiency factor	Calculation	Value
$\eta_{\text{trans}}$	no switch, 0.2 m $\Omega$ cap ESR	0.96
$\eta_{\text{sheath}}$	$1 - \frac{8 \phi_i}{V}$	0.92
$\eta_{\text{ff}}$	$1 - \frac{3 \phi_i}{V}$	0.97
$\eta_{\text{div}}$	half angle = 15 deg	0.96
$\eta_{\text{dist}}$	10% neutrals	0.90
$\eta_t$	$\eta_{\text{trans}} \eta_{\text{sheath}} \eta_{\text{ff}} \eta_{\text{div}} \eta_{\text{dist}}$	<b>0.73</b>
$\eta$	$\eta_{\text{ppu}} = 0.95$	<b>0.70</b>

TABLE III: Comparison of high-power thruster types.

Thruster type	Acceleration mechanism	$I_{sp}$ [sec]	$T/A$ [N/m <sup>2</sup> ]	$A$ [m <sup>2</sup> ] 1 MW
Ion	E-field	4,000	5	10
Hall	E,B-fields	4,000	5	10
MPD, EM	$\mathbf{j} \times \mathbf{B}$	4,000	150	0.3
PIT, EM	$\mathbf{j} \times \mathbf{B}$	4,000	50	1.0
H <sub>2</sub> Arcjet	pressure	1,000	150	0.3

### B. Thrust Density

For MW-class electric propulsion, the thrust-density (N/m<sup>2</sup>) becomes an important consideration. A comparison of thrust-densities and thrust areas for several different high-power systems operating at a baseline of 1 MW are shown in Table III. While ion and Hall thrusters require  $\sim 10$  m<sup>2</sup> per MW, electromagnetic thrusters such as the MPD and PIT are considerably smaller. Though the arcjet is also small, its specific impulse is only 1000 seconds.

### C. Heuristic Particle Description

In an attempt to gain additional insight into the acceleration process, we present a qualitative description of the plasmadynamics in a deflagration-mode GEM thruster. We assume that the electrode structure is coaxial and that the plasma has reached equilibrium, is azimuthally symmetric and does not vary in time. We further assume the plasma is 100% ionized and has a temperature of  $\sim 1.5$  eV. Two cases are presented; that for which the central electrode is the cathode (normal polarity) and the anode (reversed polarity).

Since ions carry the momentum, it is important to try and understand the ion acceleration mechanism. Ultimately, the ions gain energy from and are accelerated by, the electric field. For normal polarity, as described by Jahn[27], ions that form near the outer anode are accelerated radially inward and deflected downstream by the  $e\mathbf{u}_i \times \mathbf{B}$  force. For reversed polarity, ions are generated near the central electrode and similarly turned downstream.

The difference between normal and reversed polarity is that in the former, the ion enters the region of strong  $B$ -field as it is accelerated radially inward by the radial electric field. For the reverse case the ion is created in the region of strong  $B$ -field, possessing a smaller Larmor radius and turning downstream more easily because its radial velocity is not nearly as high as in the normal polarity case.

The other important factor in determining the ion trajectory is the axial electric field, Fig. 4. For a thruster with a long outer electrode and a short central electrode,  $E_z$  along the axis opposes the ion motion in the normal polarity case, but is in the same direction as the exhaust velocity vector when polarity is reversed. Finally, in either case, the

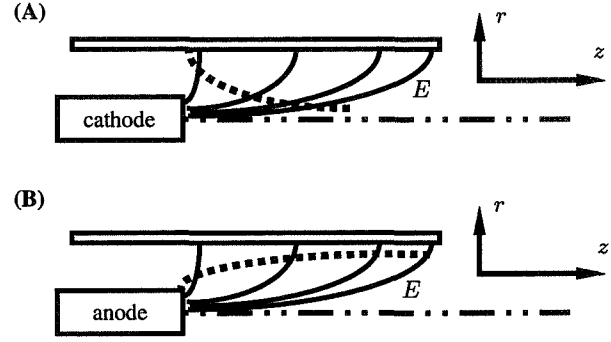


FIG. 4: Schematic showing ion trajectories (dotted lines) for when the central electrode is (A) the cathode and (B) the anode.

boundary condition that  $E$  is perpendicular to the conducting outer electrode reduces  $E_z$  to zero in the outer regions.

While MPD thrusters are typically operated with a central cathode (normal polarity), reversed polarity has also been used successfully in the coaxial Teflon pulsed plasma thruster (PPT) in conjunction with a spark ignition system[28] and in an ablative Z-pinch PPT[29]. In the coaxial PPT, propellant is fed around the central electrode and highly ionized, which is quite similar to the expected propellant injection pattern in a reversed polarity GEM thruster.

### D. Onset and the GEM Thruster

A discussion of a deflagration-mode GEM thruster would not be complete without addressing the onset issue. Onset in EM thrusters refers to the onset of high frequency terminal voltage oscillations, accompanied by high electrode erosion, when the thruster current is raised above a certain threshold (onset current) while maintaining a fixed mass flow rate. This phenomenon has been observed in nitrogen and argon-fed MPD thrusters[24, 30].

While a number of onset theories have been proposed over the last 30 years, no general agreement exists as to the mechanism, and we will not attempt to present a preferred theory here. However, we can empirically estimate onset using the nitrogen and argon MPD results. The basis for this empirical prediction is the assumption that the onset current is proportional to the number of available charge carriers. If the propellant is singly and fully ionized, the charge-carrier (C-C) fraction is

$$\phi = \frac{e \dot{m}}{N m I^*},$$

where where  $N$  is 2 for nitrogen and 1 for argon and gallium,  $m$  is the ion mass,  $\dot{m}$  is the mass flow rate and  $I^*$  is current at onset.

Table IV is a self-consistent calculation showing that, at onset, ions in nitrogen and argon MPDs carry 52-64% of the discharge current. If we adopt the average, 58%, for



TABLE IV: Comparison of onset currents for different propellants. The value of  $I^*$  for gallium is predicted based on the average value of  $\phi$  given.

Propellant	Pulse Power [MW]	$\dot{m}$ [gm/s]	$I_{sp}$ [s]	$\phi$	$I^*$ [kA]
Nitrogen	4.1	3.7	4150	0.52	21
Argon	8.1	5.6	2060	0.64	24
Gallium	12.3	20.7	3000	0.58	49

gallium, then the predicted onset current is  $I_{Ga}^* = 49$  kA (at 3000 s). Since the current is higher and more voltage is required to accelerate the more massive gallium ions, the pulse power is greater than for nitrogen or argon. To produce a 12.3 MW pulse for 100  $\mu$ s requires 1200 J/pulse, resulting in a thruster processing 120 kW of power when operating at 100 hertz. At this power level, the thrust is 6.2 N. Furthermore, a thruster that is 20 cm in diameter will possess a thrust per unit area of  $\sim 150$  N/m<sup>2</sup>. While these estimates for a GEM thruster must be validated by experiment, the extensive past work with the Ar and N<sub>2</sub> propellants allow for a level of confidence in the predictions.

#### IV. EXPERIMENTAL APPARATUS

A two-stage, pulsed GEM accelerator is presently under construction at UIUC and MSFC. The stages of the accelerator are not optimized as the hardware is designed for to allow for diagnostic access to evaluate and validate several of the potential advantages of using gallium as a propellant in a PPT.

##### A. First Stage

The GEM thruster feed system and first stage must inject gallium plasma, with mass bits of  $\sim 100$ -200 g, into the second accelerator stage at a rate up to 100 Hz. As described

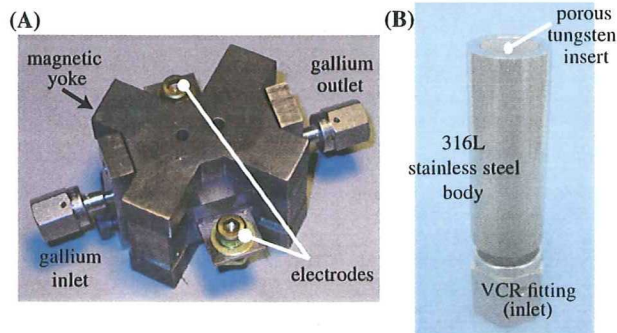


FIG. 5: (A) Liquid gallium electromagnetic pump. (B) Sintered-tungsten gallium cathode.

earlier and illustrated in Fig. 2, we use an ablative liquid-gallium-coated electrode for propellant injection.

Liquid gallium is delivered to the first stage using an electromagnetic (EM) pump, like those described in Ref. [13] and illustrated in Fig. 5A. Liquid metal enters the pump through a tube fitting and electrically shorts two electrodes on opposing sides of the pump. Two samarium-cobalt permanent magnets are located at the top and bottom of the pump, providing a strong magnetic field ( $\sim 0.2$  Tesla) through the liquid metal, transverse to the two electrodes. The pump is shrouded in a soft iron yoke, which both confines and strengthens the magnetic field inside the pump. When voltage is applied between the two electrodes, current flows through the liquid metal, transverse to the applied magnetic field, imparting a Lorentz force on the fluid, which causes it to flow in the direction of  $\mathbf{j} \times \mathbf{B}$ . Pumping gallium approximately 3 cm above its equilibrium height using the pump shown in Fig. 5A requires an applied voltage of about 0.1 V and current levels of approximately 10 A. The total pump power input is generally on the order of a few watts, making it a minimal burden on high-power systems. An EM pump based liquid metal feed system also does not require pressurized gas, valves, or other moving parts, enabling a compact, robust feed system for both laboratory testing and implementation on spacecraft.

The feed system forces liquid gallium into the porous metal electrode (Fig. 5B). Capillary forces draw the gallium through the metal matrix, to the surface, where it forms a thin surface layer above the underlying material (porous tungsten, for example). The pumping rate is adjusted to continually compensate for the loss of material from the ablative action of the first stage arc discharge.

We can estimate a few elements of the energy budget that will be required to evaporate enough gallium to match the second stage mass bits. We assume that (prior to contact with the arc discharge) the gallium surface temperature is 500 K (2000 K below its boiling temperature). Also, if we expect the plasma temperature to be approximately 1 eV or higher, the equilibrium mole fraction plot (Fig. 1) indicates that the propellant will be completely singly ionized. Allowing for other losses in the system, a first stage energy of about 25-50 J/pulse is adequate to provide the required mass for low  $I_{sp}$  operation of the GEM thruster. During the high  $I_{sp}$  phases of operation, the first stage will be able to operate at about 10 J/pulse. In either case, the power requirements for the first stage will be small - less than five percent of the second stage.

##### B. Pulser

The pulser provides the energy to evaporate and heat the gallium in the first stage. For short pulses, an SCR-switched capacitor discharging into the first stage is sufficient. In Fig. 6 is a 20 J, 20 Hz (400 W) unit that provides a fast-rising, non-reversing current pulse with a low-inductance circuit containing a free-wheeling diode. The repetition rate of this pulser must be raised to  $\sim 100$  Hz for



high power operation.

### C. Second Stage

The second stage we have constructed at MSFC is shown in Fig. 7. Its cathode and anode are fabricated from copper. The cathode has an outer radius of 7.6 cm, a length of 7.6 cm and a 2.5 cm hole running down its centerline. The anode has an inner diameter of 20.3 cm and a length of 48.3 cm. At the breach the anode connects to a copper back-plate that has a 15.2 cm hole aligned with the accelerator's centerline. The cathode-anode gap at the breach is covered with a Macor plate.

Four high-energy Maxwell capacitors with a capacitance of 15  $\mu\text{F}$  each are connected in parallel across the cathode and anode. The system is designed for a charge voltage of 20 kV, resulting in an energy of 12 kJ per pulse. The capacitors are charged using a General Atomics 112 kJ/s power

supply, which is protected from current ringing by a set of nine flyback diodes connected in series. The discharge is triggered when gas is injected into the accelerator through the hole in the cathode, bringing the pressure in the discharge chamber to a high enough level to allow for current to flow between the two electrodes.

The second stage is intended to test the effectiveness of injecting a preionized gallium plasma for current switching. This will be performed by comparing current waveforms and  $B$ -dot probe measurements from within the plasma to analogous data obtained when the injected propellant is a neutral gas (argon, for example). We can also spectroscopically quantify the electrode erosion in the thruster for both gallium and argon to evaluate the effect gallium has on electrode erosion. Finally, a systematic campaign to map the time-varying magnetic field in the discharge chamber will help to confirm or dispel our intuition regarding current sheet motion and propellant acceleration in a short pulse-length GEM thruster.

### V. CONCLUSIONS

We have hypothesized that there are advantages to using gallium as a propellant in an electromagnetic accelerator, supported by empirical and heuristic analyses. Such a thruster could have the following beneficial or advantageous properties.

- The non-toxic propellant would be easier to handle and store relative to other liquid metal thruster systems, such as lithium, cesium or mercury.
- The use of gallium could mitigate several critical issues that presently limit the development of high-current, high-power pulsed plasma accelerators. The most important of these concern pulsed mass injection, pulsed power switching, and electrode erosion.
- Gallium's high atomic mass and low ionization potential implies high efficiency operation. The thrust efficiency for a GEM thruster operating in the deflagration mode could be as high as 70%.
- Gallium atoms may be more easily accelerated in a GEM thruster where the inner electrode was the anode.
- It may be possible to operate a gallium-fed thruster at much higher current and power levels than past MPD thrusters before reaching onset.

The first stage of a two-stage GEM thruster is presently under construction at UIUC to test issues related to liquid gallium propellant management and pulsed mass injection. The second stage, constructed at MSFC, will be used to evaluate pulsed power switching using an ionized gallium plasma and provide information regarding the time-evolution of the current pattern in the thruster.

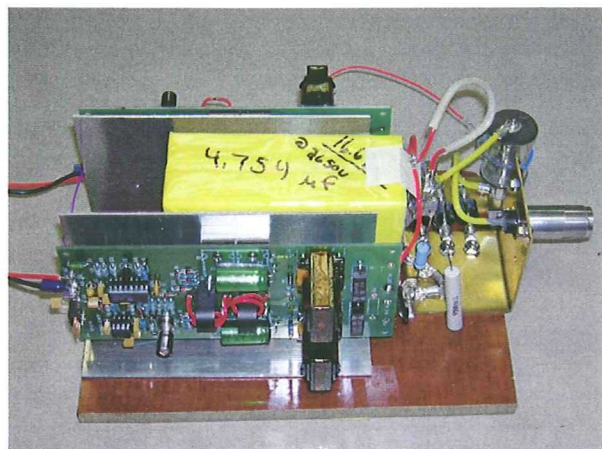


FIG. 6: First Stage 20 J, 20 Hz pulser for low  $I_{sp}$  operation.

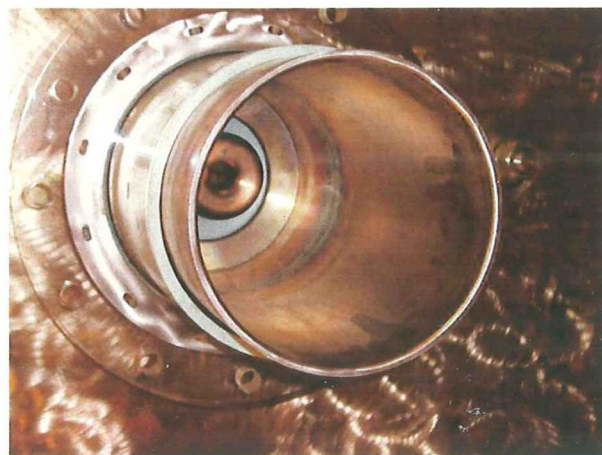


FIG. 7: Photograph looking down the barrel of MSFC's GEM thruster.



### Acknowledgments

The UIUC co-authors acknowledge support from the Alabama NASA Space Grant Consortium through the University of Alabama at Huntsville, the NASA Graduate Student Research Program through the NASA Marshall Space Flight Center, and the UIUC Center for Space Technology and Research (CSTAR). We greatly appreciate discussions

with John Frus at GE/Unison Industries, Jacksonville, FL.

The MSFC co-authors appreciate the management support of Mike Fazah and Jim Martin and the program office support of Dr. Michael LaPointe. We also acknowledge the contributions of Doug Galloway, Tommy Reid, and Amado DeHoyos. This work was partially supported through an MSFC Center Director Discretionary Funds (CDDF) research award.

- [1] D.J. Connolly, R.J. Sovie, C.J. Michels, and J.A. Burkhart. "Low environmental pressure MPD arc tests". *AIAA J.*, 6(7):1271, 1968.
- [2] A.D. Kodys, G. Emsellem, L.D. Cassady, J.E. Polk, and E.Y. Choueiri. "Lithium mass flow control for high power Lorentz force accelerators". In *Proc. Space Tech. and International Forum (STAIF) 2001*, AIP Conf. Proc.
- [3] H.J. King, J.H. Molitor, and S. Kami. "System concepts for a liquid mercury cathode thruster". Sept. 1967. AIAA 1967-699.
- [4] J. Hyman Jr., J.R. Bayless, D.E. Schnelker, J.W. Ward, and J. Simpkins. "Development of a liquid-mercury cathode thruster system". *J. Spacecraft Rockets*, 8(7):717, 1971.
- [5] C.R. Collett, C.R. Dulgeroff, and J.M. Simpkins. "Cesium microthruster system". Mar. 1969. AIAA 1969-292.
- [6] S. Marcuccio, A. Genovese, and M. Andreucci. "Experimental performance of field emission microthrusters". *J. Propuls. Power*, 14(5):774, 1998.
- [7] M. Tajmar, A. Genovese, and W. Steiger. "Indium field emission electric propulsion microthruster experimental characterization". *J. Propuls. Power*, 20(2):211, 2004.
- [8] S.O. Tverdokhlebov, A.V. Semenko, and J.E. Polk. "Bismuth propellant option for very high power TAL thruster". *40th AIAA Aerospace Sciences Meeting*, Jan. 14-17, 2002. AIAA Paper 2002-348.
- [9] A. Sengupta, *et al.* "An overview of the VHITAL program: a two-stage bismuth fed very high specific impulse thruster with anode layer". *29th International Electric Propulsion Conference*, Princeton, NJ, Oct. 31-Nov. 4, 2005.
- [10] J. Szabo, C. Gasdaska, V. Hruby, and M. Robin. "Bismuth Hall thruster with ceramic discharge channel". *Proc. 53rd JANNAF Propulsion Meeting*, Monterey, CA, Dec. 2005.
- [11] T.E. Markusic, Y.C.F. Thio, and J.T. Cassibry. "Design of a high-energy, two-stage pulsed plasma thruster". *38th AIAA/ASME/SE/ASEE Joint Propulsion Conference*, July 7-10, 2002. AIAA Paper 2002-4125.
- [12] T.E. Markusic. "Liquid-metal-fed pulsed electromagnetic thrusters for in-space propulsion". *Proc. 52nd JANNAF Propulsion Meeting*, Las Vegas, NV, May 2004.
- [13] T.E. Markusic, K.A. Polzin, and A. DeHoyos. "Electromagnetic pumps for conductive-propellant feed systems". *29th International Electric Propulsion Conference*, Princeton, NJ, Oct. 31-Nov. 4, 2005.
- [14] R.L. Burton and P.J. Turchi. "Pulsed plasma thruster". *J. Propuls. Power*, 14(5):716-735, Sept.-Oct. 1998.
- [15] J. Marshall. "Performance of a hydromagnetic plasma gun". *Phys. Fluids*, 3(1):134-135, 1966.
- [16] T.L. Rosenbrock *et al.* "Pulsed electromagnetic acceleration of metal plasmas". *AIAA J.*, 2:328, 1964.
- [17] P. Gloersen, B. Gorowitz, and J.H. Rowe. "Some characteristics of a two-stage repetitively fired coaxial gun". *IEEE Trans. Nuclear Sci.*, pages 249-265, 1964.
- [18] B. Gorowitz, T.W. Karras, and P. Gloersen. "Performance of an electrically triggered repetitively pulsed coaxial plasma engine". *AIAA J.*, 4(6):1027-1031, 1966.
- [19] T.W. Karras, B. Gorowitz, and P. Gloersen. "Experimentally measured velocity distribution in the plasma stream of a pulsed coaxial accelerator". *Phys. Fluids*, 9(9):1874-1876, 1966.
- [20] P.J. Turchi, C.N. Boyer, and J.F. Davis. "Multi-stage plasma propulsion". *17th International Electric Propulsion Conference*, Tokyo, Japan, May 28-31, 1984. IEPC-84-51.
- [21] L.A. Gomilka, A.I. Zemskov, L.N. Lesnevskii, and A.D. Pavlov. "A study of the plasma pulsed accelerator with the metallic propellants". *24th IAF International Astronautical Conference*, Baku, Azerbaidzhan SSR, Oct., 1973. Paper #7-13.
- [22] C.L. Dailey and R.H. Lovberg. *The PIT MkV pulsed inductive thruster*. Technical Report NASA CR-191155, TRW Systems Group, July 1993.
- [23] D.-Y. Chang and C.N. Chang. "Deflagration plasma thruster". In *Progress in Aeronautics and Astronautics*, edited by L.H. Caveny, Vol. 89, AIAA, Reston, VA, 1984.
- [24] R.L. Burton, K.E. Clark, and R.G. Jahn. "Measured performance of a multimewatt MPD thruster". *J. Spacecraft*, 20(3):299-304, May-June 1983.
- [25] R.L. Burton, F. Rysanek, E.A. Antonsen, M.J. Wilson, and S.S. Bushman. "Pulsed plasma thruster performance for microspacecraft propulsion". In *Micropropulsion for Small Spacecraft*, Ch. 13, edited by M.M. Micci and A.D. Ketsdever, Vol. 187, Progress in Aeronautics and Astronautics, AIAA, Reston, VA, 2000, pp. 337-352.
- [26] N.T. Tiliakos and R.L. Burton. "Arcjet anode sheath voltage measurements by Langmuir probes". *J. Propuls. Power*, 12(6):1174-1176, Nov.-Dec. 1996.
- [27] R.G. Jahn. *Physics of Electric Propulsion*. McGraw-Hill Book Company, 1968.
- [28] J. Laystrom and R.L. Burton. "Geometric optimization of a coaxial pulsed plasma thruster". In *39th AIAA/ASME/SAE/ASEE Joint Propulsion Conference*, Huntsville, AL, July 20-23 2003. AIAA 2003-5025.
- [29] T.E. Markusic, K.A. Polzin, E.Y. Choueiri, M. Keidar, I.D. Boyd, and N. Lepsetz. "Ablative Z-pinch pulsed plasma thruster". *J. Propuls. Power*, 21(3):392-400, May-June 2002.
- [30] J.K. Ziemer and E.Y. Choueiri. "Quasi-steady magnetoplasma dynamic thruster performance database". *J. Propuls. Power*, 17(5):520-529, Sept.-Oct. 2001.